IEEE Photonics Journal
An IEEE Photonics Society Publication

Open Access

Enhancing Secrecy Capacity in FSO Links via MISO Systems Through Turbulence-Induced Fading Channels With Misalignment Errors

Volume 12, Number 4, August 2020

Rubén Boluda-Ruiz
Sezer Can Tokgoz
Antonio García-Zambrana
Khalid Qaraqe

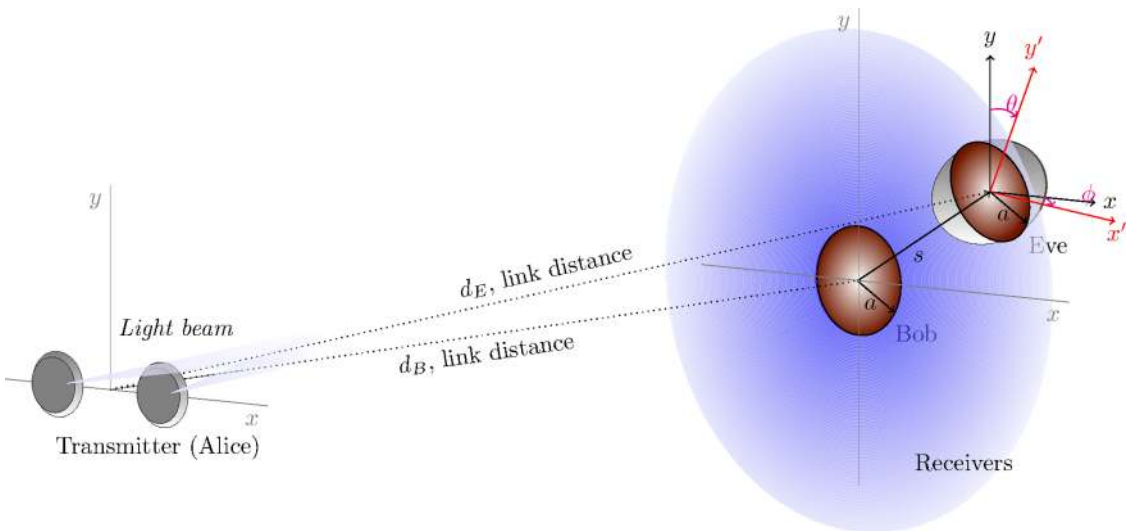

DOI: 10.1109/JPHOT.2020.2987378

Enhancing Secrecy Capacity in FSO Links via MISO Systems Through Turbulence-Induced Fading Channels With Misalignment Errors

Rubén Boluda-Ruiz,[1] **Sezer Can Tokgoz**,[1] **Antonio García-Zambrana**,[2] **and Khalid Qaraqe**[1]

[1]Department of Electrical and Computer Engineering, Texas A&M University at Qatar, Doha 23874, Qatar
[2]Andalucía Tech, Department of Communications Engineering, Campus de Teatinos, University of Málaga, Málaga 29701, Spain

DOI:10.1109/JPHOT.2020.2987378

Manuscript received November 26, 2019; revised April 2, 2020; accepted April 8, 2020. Date of publication April 17, 2020; date of current version June 10, 2020. This work was supported in part by TAMUQ 2019 RRSG internal funds and by National Priorities Research Program under Grant NPRP12S-0225-190152 from the Qatar National Research Fund [a member of Qatar Foundation (QF)]. This article was presented in part at the 20th IEEE International Workshop on Signal Processing Advances in Wireless Communications, Cannes, France, Jul. 2019. Corresponding author: Rubén Boluda-Ruiz (e-mail: ruben.boluda_ruiz@qatar.tamu.edu).

Abstract: It has recently been proved that the free-space optical (FSO) communication links are susceptible to interceptions. Due to this reason, the optics community shows a special interest in studying these high-speed links in greater detail from a physical layer security (PLS) point of view. Therefore, in this paper, we propose, for the first time, enhancing the average secrecy capacity (ASC) in FSO links via multiple-input/single-output (MISO) systems. It is well-known that the fading effects in FSO channels can be significantly mitigated by exploiting spatial diversity techniques at the transmitter end. Thus, we develop a new asymptotic closed-form solution at high signal-to-noise-ratio (SNR) to accurately compute the ASC for MISO based FSO communication systems with equal gain combining (EGC) reception through generalized misalignment and atmospheric turbulence-induced fading channels. As a key feature, we investigate the impact of the eavesdropper's orientation along with its location in the pointing error model. We can conclude that the influence of the eavesdropper on recollecting radiated power is diminished considerably by increasing not only the normalized beam width at the receiver end, but also by increasing the number of laser sources. Numerical results are tested by exact Monte Carlo simulations.

Index Terms: Free-space optical (FSO), physical layer security (PLS), average secrecy capacity (ASC), atmospheric turbulence, multiple-input/multiple-output (MIMO), equal gain combining (EGC).

1. Introduction

1.1 Motivation

In the present-days, many researchers try to give answer the question of how to guarantee the security of confidential messages in advanced wireless communication systems and communication services for the emerging implementation of 5G and beyond wireless networks [2]. There is an

urgent need from both academia and industry for exploring the fundamental information-theoretic security limits. Physical layer security (PLS) has been considered as an attractive research field to complement traditional encryption methods [3], [4]. The main reason to consider PLS is to renounce a part of the data rate to combat eavesdropping by utilizing the inherent randomness of the physical communication media.

Over the last few decades, many interesting articles have been reported from the information-theoretic security point of view, especially in radio-frequency (RF) systems [5]–[8] (and references therein), which provide comprehensive analysis to notably improve the PLS through fading channels in terms of the secrecy outage probability (SOP) and the average secrecy capacity (ASC) via multiple-input/multiple-output (MIMO) systems, cooperative communication and cognitive networks, among others. According to the great improvement achieved in PLS aspects of RF systems by MIMO techniques, it is expected that this kind of transmission also presents a remarkably impact on PLS aspects related to optical wireless communication systems.

1.2 Related Works

Due to the fact that the RF spectrum is suffering from a serious congestion, free-space optical (FSO) communication systems have been extensively studied over the past decade as an attractive alternative technology to RF since they are promising candidates for emerging broadband technologies for the next generation networks [9]. Recently, it has been demonstrated that FSO technology is not interception-free [10]. Motivated by that, they are currently being investigated from the perspective of PLS [11]–[16]. Hence, the real interest of the optics community is to improve the maximum achievable data rate with a secrecy limitation that these systems are capable of achieving through atmospheric turbulence channels with misalignment errors in the presence of an external observer with arbitrary orientation and location.

As it is well-known, FSO communication systems are severely degraded by fading, which is mainly produced by atmospheric scintillation because of microvariations in the refractive-index through the FSO link and misalignment errors between the transmitter and the receiver produced by external agents that result in building sways [9], [17]–[19]. Thus, the fading effects of FSO channels can be significantly mitigated by using multiple-input/single-output (MISO) FSO systems based on spatial diversity methods with multiple lasers at the transmitter end [20]. In this paper, we employ, for the first time, diversity techniques to improve PLS in FSO communication systems. To the best of our knowledge, the inherent benefits of diversity methods to enhance the achievable secrecy rate have not been fully exploited yet. In this sense, there is still an open research problem for the study of ASC performance of MISO FSO systems by including the impact of an external observer with arbitrary orientation and location. The deployment of MISO FSO systems is expected to result in an attractive and promising approach to reduce potential wiretapper's attacks as well as the security flaws in the physical layer.

1.3 Main Contributions

In this research, we propose to enhance the ASC performance for MISO based FSO communication systems in order to fill some gaps in the existing literature. The main contributions of this research are summarized as follows:

- We present a new asymptotic closed-form solution for the ASC of MISO based FSO systems, which employs equal gain combining (EGC) reception through gamma-gamma (GG) atmospheric turbulence channels with nonzero boresight pointing errors. This asymptotic solution proved to be very useful and accurate to compute the secrecy performance.
- As a key feature, we pay special attention to the eavesdropper's location and its orientation since it makes sense to assume that the eavesdropper is not located in the line-of-sight of the legitimate pairs. Thus, the eavesdropper is able to capture a fraction of radiated power, depending on its location and orientation.

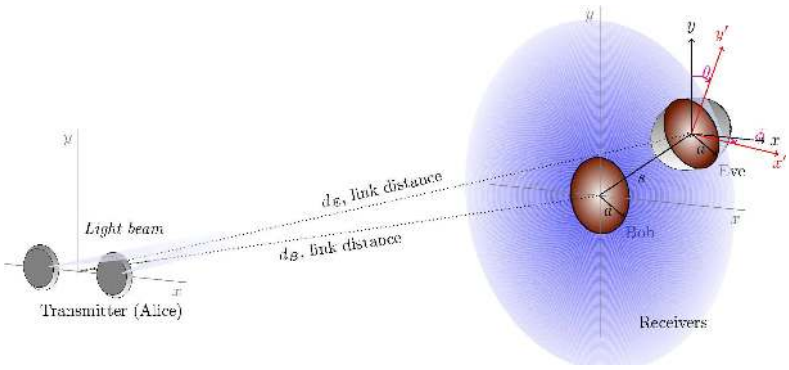

Fig. 1. MISO FSO system under study, where s represents the eavesdropper's location in the xy-plane, and the angles θ and ϕ represent the eavesdropper's orientation in x-axis and y-axis, respectively. As an example, we depict in this figure a MISO FSO communication system with $M = 2$ for a source-destination link distance of d_B. Note that the two laser sources are aligned with the main receiver Bob.

- We use the developed expression for the ASC, which is tested through exact Monte Carlo simulations for different atmospheric turbulence conditions in the presence of pointing errors, to understand the impact of some influential parameters such as the number of laser sources employed at the transmitter end, the normalized beam width area at the receiver end, the SNR of the eavesdropper's link, and the eavesdropper's location and orientation on the ASC performance.
- Unlike the current literature [14]–[16], where MISO FSO systems have not been employed yet, we can conclude that a higher secrecy rate is achievable at several eavesdropper locations over different turbulent conditions when the number of employed laser sources is greater than one at the transmitter end.

1.4 Organization

The rest of this work is arranged as follows. In Section 2, we describe the system and channel models. In Section 3, we conduct the asymptotic ASC performance analysis. In Section 4, we use the developed asymptotic solution for the ASC to show some numerical results and, then we finally provide some concluding remarks in Section 5.

2. System and Channel Models

As shown in Fig. 1, the FSO scenario under study is being considered in recent papers related to PLS for FSO communication where the use of technology based on intensity-modulation and direct-detection (IM/DD) is used for deploying terrestrial FSO links due to its low cost and simplicity. Thus, one potential PLS attack will occur when Eve falls within the divergence area of the optical beam because of the effect of atmospheric turbulence. In practice, this results in that Eve is installed close to Bob, i.e. they are placed in the top of the same building, as depicted in Fig. 1. As usually considered in the deployment of terrestrial FSO links [21], we assume here that Bob, Alice and Eve are fixed devices. The potential risk of eavesdropping would be even more significant in urban communications where an eavesdropper may be hidden in a nearby window [10], or in satellite-to-ground laser communications in which the beam footprint could be at the order of kilometers. Also, note that for long FSO distances between Alice and Bob, Eve would have a greater chance for eavesdropping by capturing radiated power. Due to the fact that the atmospheric coherence length, which is defined as $r_0 = 1.65(C_n^2(2\pi/\lambda)^2 d_m)^{-3/5}$, is on the order of centimeters, we assume FSO channels statistically independent [22].

TABLE 1
FSO Communication System Setup

Parameter	Symbol	Value
Wavelength	λ	1550 nm
FSO link distance	d_m	{3,4} km
Receiver aperture diameter	$D_m = 2a$	10 cm
Number of transmitters	M	{1,2,4,6}
Normalized beam width	ω_z/a	{6,10}
Normalized standard deviation	σ_s/a	{1,2}
Eavesdropper's location	$(\mu_x/a, \mu_y/a)$	{(6,2),(8,4)}
Eavesdropper's orientation	ρ/a	{0.6, 0.9}
Moderate turbulence conditions		
Haze visibility	V	4 km
Structure parameter	C_n^2	$2 \times 10^{-14}\ m^{-2/3}$
Rytov variance	σ_R^2	3
Attenuation	L_m	0.346
Strong turbulence conditions		
Clear visibility	V	16 km
Structure parameter	C_n^2	$8 \times 10^{-14}\ m^{-2/3}$
Rytov variance	σ_R^2	12
Attenuation	L_m	0.826

The received electrical SNR for the MISO FSO system shown in Fig. 1 is given by

$$SNR(h_{m_T}) = \frac{1}{2}\frac{(2P_t/M)^2}{\sigma_n^2}\left(\sum_{k=1}^{M} h_{m_k}\right)^2 = 4\frac{P_t^2}{M^2 N_0} h_{m_T}^2 = 4\frac{\gamma_m}{M^2} h_{m_T}^2, \tag{1}$$

where h_{m_T} is the resulting channel gain, P_t is the average transmitted optical power, $\sigma_n^2 = N_0/2$ is the noise at the receiver which is modeled as additive white Gaussian noise (AWGN) with zero mean, $\gamma_m = P_t^2 R^2/N_0$ is the transmit SNR with no turbulence-induced fading, and m denotes E for Eve and B for Bob. The FSO channel gain, h_{m_k}, is defined as $h_{m_k} = L_m \cdot h_a \cdot h_p$, where L_m is the atmospheric attenuation, h_a is the turbulence-induced fading, and h_p is the pointing error at the receiver-side. Note that L_m is determined by the Beer Lambert's law as $L_m = e^{-\Phi d_m}$, with d_m being the FSO link distance and Φ the atmospheric attenuation coefficient [23].

2.1 Statistical Modeling of Pointing Errors

Let us assume here a pointing error model, where the optical beam is non-orthogonal with respect to the receiver plane, i.e., the eavesdropper's receiver is rotated by an angle θ in x-axis, and by an angle ϕ in the y-axis. Thus, the corresponding PDF of this pointing error model is expressed as in [16, Eq. (7)] as follows

$$f_{h_p}^{\text{Eve}}(h) \simeq \frac{\varphi_E^2}{A_E^{\varphi_E^2}} h^{\varphi_E^2 - 1}, \quad 0 \le h \le A_E, \tag{2}$$

where $A_0 = [\text{erf}(v_E)]^2$ is the fraction of the collected power at $r_E = 0$, $v_E = \sqrt{\pi a^2 \cos\theta \cos\phi}/\sqrt{2}\omega_z$, $\omega_{z_{eqE}}^2 = \omega_z^2 \sqrt{\pi}\,\text{erf}(v_E)/2v_E \exp(-v_E^2)$ is the equivalent beam width, $\sigma_E^2 = ((3/2)\sigma_s^4 s^2 + \sigma_s^6)^{1/3}$ [18, Eq. (9)], and $\varphi_E = \omega_{z_{eqE}}/2\sigma_E$. Besides, the parameter A_E was computed in [16, Eq. (8)]. In relation to the pointing error modeling of Bob, this one is a particular case of the previous one, where $\rho/a = 1$ (Bob is not rotated), and the same jitter variances ($\sigma_x = \sigma_y = \sigma_s$) and a zero boresight displacement ($\mu_x = \mu_y = 0$) are considered.

Finally, the PDF of the FSO communication link when the atmospheric turbulence follows the GG model of parameters α_m and β_m [17] and the misalignment error follows a modified Rayleigh

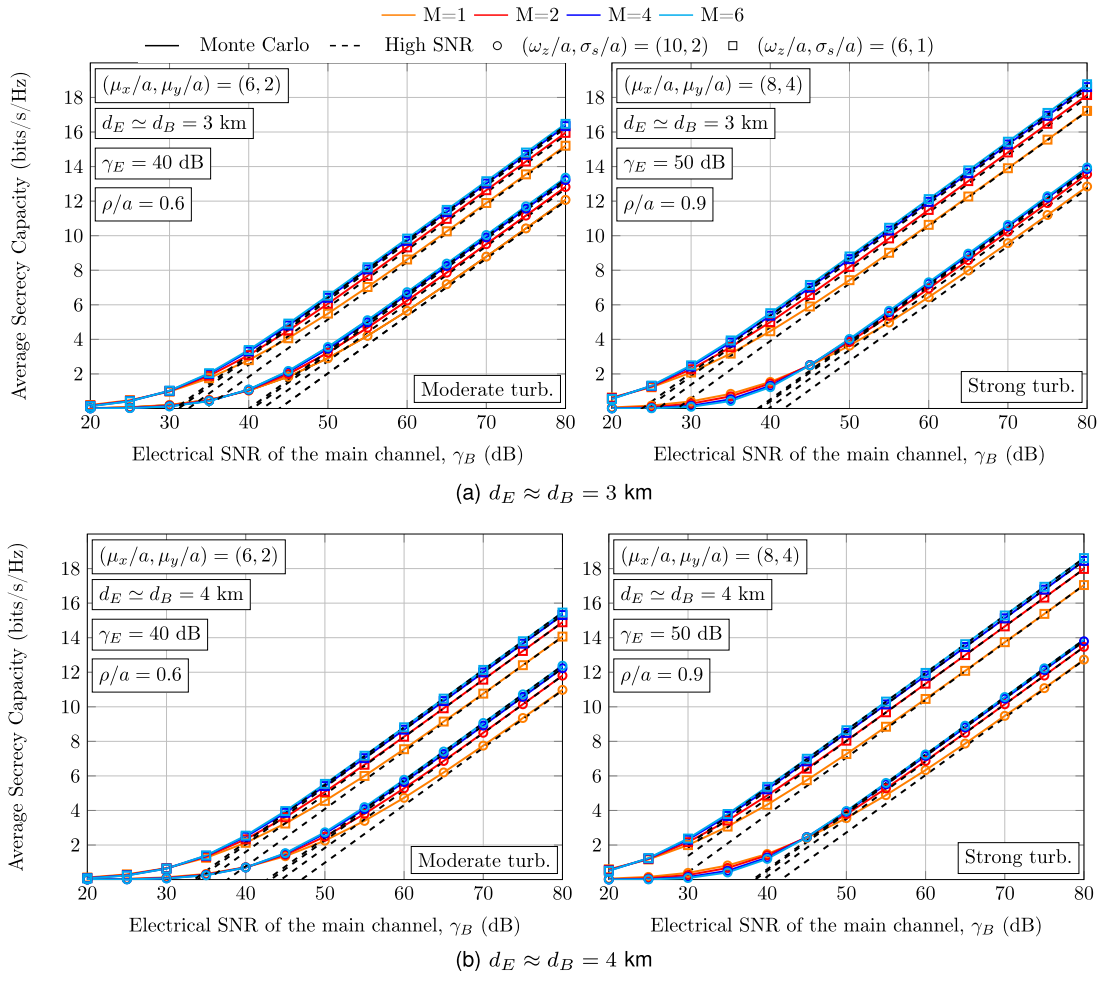

Fig. 2. ASC of MISO FSO communication systems for an FSO link distance of (a) 3 km, and (b) 4 km as a function of γ_B for different severity of misalignment errors under different weather and turbulent conditions when different eavesdropper's locations are considered.

distribution is determined as in [18] as follows

$$f_{h_{m_k}}(h) = \frac{\varphi_m^2 h^{-1}}{\Gamma(\alpha_m)\Gamma(\beta_m)} G_{1,3}^{3,0}\left[\frac{\alpha_m \beta_m}{A_m L_m} h \,\middle|\, \begin{matrix} \varphi_m^2 + 1 \\ \varphi_m^2, \alpha_m, \beta_m \end{matrix}\right], \tag{3}$$

where $G_{p,q}^{m,n}[\cdot]$ is the Meijer's G-function [24, Eq. (8.2.1)]. When plane wave propagation is considered, α_m and β_m are obtained as in [25].

3. Asymptotic ASC Analysis for MISO Wiretap Channels

According to the information-theoretic formulation [3], the ASC is the maximum achievable secrecy rate, which is defined as follows

$$C_s = [C_B - C_E]^+ = B\left[\log_2\left(1 + 4\frac{\gamma_B}{M^2} h_{B_T}^2\right) - \log_2\left(1 + 4\frac{\gamma_E}{M^2} h_{E_T}^2\right)\right]^+, \tag{4}$$

where $[x]^+ = \max(x, 0)$, B is the channel bandwidth, C_B denotes the ergodic capacity between the legitimate peers (Alice-Bob), and C_E denotes the ergodic capacity of the eavesdropper's channel

(Alice-Eve). In this analysis, we compute the ASC as in [5, Eq. (15)] as follows

$$C_s = B\frac{8\gamma_E}{\ln(2)}\int_0^\infty \frac{h_{E_T}}{\left(1+4\frac{\gamma_E}{M^2}h_{E_T}^2\right)} F_{h_{E_T}}(h_{E_T})\left[1-F_{h_{B_T}}\left(h_{E_T}\sqrt{\frac{\gamma_E}{\gamma_B}}\right)\right]dh_{E_T}, \tag{5}$$

where $F_{h_{m_T}}(h)$ is the cumulative distribution function (CDF) of the resulting channel gain of h_{m_T}. To the best of our knowledge, expressing the above integral in closed-form could be quite a challenging, if not impossible, for the MISO FSO wiretap channel model considered here. However, an asymptotic analysis can be carried out at high SNR in order to analyze the improvement in security issues by employing MISO FSO structures through turbulence-induced fading channels. Hence, the ASC of MISO FSO systems is obtained by averaging Eq. (4) over the PDFs as follows

$$C_s = \int_0^\infty \int_0^\infty [C_B - C_E]^+ f_{h_{B_T}}(h_{B_T}) f_{h_{E_T}}(h_{E_T}) dh_{B_T} dh_{E_T}. \tag{6}$$

By performing some easy algebraic manipulations, the above equation can be written as

$$\begin{aligned} C_s/B = \bar{C}_s = &\frac{1}{\ln 2}\int_0^\infty \ln\left(1+4\frac{\gamma_B}{M^2}h_{B_T}^2\right)\left[\int_0^{h_{B_T}\sqrt{\frac{\gamma_B}{\gamma_E}}} f_{h_{E_T}}(h_{E_T})dh_{E_T}\right] f_{h_{B_T}}(h_{B_T})dh_{B_T} \\ &- \frac{1}{\ln 2}\int_0^\infty \ln\left(1+4\frac{\gamma_E}{M^2}h_{E_T}^2\right)\left[\int_{h_{E_T}\sqrt{\frac{\gamma_E}{\gamma_B}}}^\infty f_{h_{B_T}}(h_{B_T})dh_{B_T}\right] f_{h_{E_T}}(h_{E_T})dh_{E_T}. \end{aligned} \tag{7}$$

By firstly solving the inner integrals, the above integral can be rewritten as

$$\begin{aligned} \bar{C}_s = &\frac{1}{\ln 2}\int_0^\infty \ln\left(1+4\frac{\gamma_B}{M^2}h_{B_T}^2\right) F_{h_{E_T}}\left(h_{B_T}\sqrt{\frac{\gamma_B}{\gamma_E}}\right) f_{h_{B_T}}(h_{B_T})dh_{B_T} \\ &- \frac{1}{\ln 2}\int_0^\infty \ln\left(1+4\frac{\gamma_E}{M^2}h_{E_T}^2\right)\left[1-F_{h_{B_T}}\left(h_{E_T}\sqrt{\frac{\gamma_E}{\gamma_B}}\right)\right] f_{h_{E_T}}(h_{E_T})dh_{E_T}. \end{aligned} \tag{8}$$

By making use of some properties of the logarithmic function, and the fact that $F_{h_{E_T}}(h_{B_T}\sqrt{\frac{\gamma_B}{\gamma_E}}) \to 1$ and $F_{h_{B_T}}(h_{E_T}\sqrt{\frac{\gamma_E}{\gamma_B}}) \to 0$ when $\gamma_B \to \infty$, we derive the asymptotic solution for the ASC as

$$\bar{C}_s \doteq \frac{1}{\ln 2}\int_0^\infty \ln\left(4\frac{\gamma_B}{M^2}h_{B_T}^2\right) f_{h_{B_T}}(h_{B_T})dh_{B_T} - \frac{1}{\ln 2}\int_0^\infty \ln\left(1+4\frac{\gamma_E}{M^2}h_{E_T}^2\right) f_{h_{E_T}}(h_{E_T})dh_{E_T}. \tag{9}$$

Note that the above equation involves the PDF of h_{m_T}, i.e. $f_{h_{m_T}}(h)$, which results in being highly complex, if not impossible, to derive its statistics. Thus, we will make use of the existing inequality among the geometric mean and the arithmetic mean to provide a lower bound (LB) expression for the PDF of the unified MISO FSO fading channel as follows

$$\frac{1}{M}\sum_{k=1}^{M} h_{m_k} \geq \sqrt[M]{\prod_{k=1}^{M} h_{m_k}}. \tag{10}$$

The above inequality can be rewritten as

$$h_{m_T} = \sum_{k=1}^{M} h_{m_k} \geq M\sqrt[M]{F_m \cdot \prod_{k=1}^{M} h_{m_k}} = M\sqrt[M]{F_m \cdot h_{m_{LB}}}. \tag{11}$$

It should be noted that $f_{h_{m_{LB}}}(h)$ permits a much easier mathematical treatment than $f_{h_{m_T}}(h)$. As can be observed from Eq. (11), there is a mismatch among the means in both sides of the above equation. To fix that, we have added a correcting factor F_m as in [22, Eq. (26)], yielding

$$F_m = \left(\frac{A_m^2 L_m^2 \varphi_m^2}{\alpha_m \beta_m\left(\varphi_m^2+1\right)}\right)^M \cdot \left(\frac{\Gamma(\alpha_m)\Gamma(\beta_m)\left(M\varphi_m^2+1\right)}{M\varphi_m^2\Gamma\left(\alpha_m+\frac{1}{M}\right)\Gamma\left(\beta_m+\frac{1}{M}\right)}\right)^{M^2}. \tag{12}$$

Now, we can obtain the PDF $f_{h_{m_{LB}}}(h)$ by making use of the inverse Mellin transform [26], yielding

$$f_{h_{m_{LB}}}(h) = \frac{\prod_{k=1}^{M} \varphi_{m_k}^2 \, G_{M,3M}^{3M,0}\left(\prod_{k=1}^{M} \frac{\alpha_{m_k}\beta_{m_k}}{A_{m_k}L_{m_k}} h \,\middle|\, \begin{matrix} \varphi_{m_1}^2+1, \ldots, \varphi_{m_M}^2+1 \\ \varphi_{m_1}^2, \alpha_{m_1}, \beta_{m_1}, \ldots, \varphi_{m_M}^2, \alpha_{m_M}, \beta_{m_M} \end{matrix} \right)}{h \prod_{k=1}^{M} \Gamma(\alpha_{m_k})\Gamma(\beta_{m_k})}. \tag{13}$$

Now, substituting Eqs. (11) and (13) into Eq. (9), we can express Eq. (9) as follows

$$\bar{C}_s \doteq \frac{\ln(4\gamma_B)}{\ln(2)} + \frac{2\ln(F_B)}{M\ln(2)} + \frac{2}{M\ln(2)} \sum_{k=1}^{M} \underbrace{\int_0^{\infty} \ln(h) f_{h_{B_k}}(h) dh}_{I_1}$$

$$- \frac{1}{\ln(2)} \underbrace{\int_0^{\infty} \ln\left(1 + 4\gamma_E \left(hF_E\right)^{\frac{2}{M}}\right) f_{h_{E_{LB}}}(h) dh}_{I_2}. \tag{14}$$

In order to solve the integral I_1, we can firstly use [27, Eq. (23)] by setting the parameter $N = 1$ and $s = 0$ for the main channel. Finally, we can express the integral I_2 in terms of the H-Fox function $H_{p,q}^{m,n}[\cdot]$ [28, Eq. (1.1)] by making use of [24, Eq. (8.4.6.5)] and [29, Eq. (07.34.21.0012.01)], yielding

$$\bar{C}_s \doteq \frac{\ln(4\gamma_B)}{\ln(2)} + \frac{2\ln(F_B)}{M\ln(2)} + \frac{1}{M\ln(2)} \sum_{k=1}^{M} \psi(\alpha_{B_k}) + \psi(\beta_{B_k}) - \frac{1}{\varphi_{B_k}^2} - \ln\left(\frac{\alpha_{B_k}\beta_{B_k}}{A_{B_k}L_{B_k}}\right)$$

$$- \frac{\prod_{k=1}^{M} \varphi_{E_k}^2 \, H_{2+3M,2+M}^{1,2+3M}\left(4\gamma_E \sqrt[M]{F_E} \left(\prod_{k=1}^{M} \frac{A_{E_k}L_{E_k}}{\alpha_{E_k}\beta_{E_k}} \right)^{\frac{2}{M}} \,\middle|\, \begin{matrix} (1,1), (1,1), \xi_1 \\ (1,1), \xi_2, (0,1) \end{matrix} \right)}{\ln(2) \prod_{k=1}^{M} \Gamma(\alpha_{E_k})\Gamma(\beta_{E_k})}, \tag{15}$$

where $\xi_1 = \{(1-\varphi_{E_1}^2, \frac{2}{M}), (1-\alpha_{E_1}, \frac{2}{M}), (1-\beta_{E_1}, \frac{2}{M}), \ldots, (1-\varphi_{E_M}^2, \frac{2}{M}), (1-\alpha_{E_M}, \frac{2}{M}), (1-\beta_{E_M}, \frac{2}{M})\}$, and $\xi_2 = \{(-\varphi_{E_1}^2, \frac{2}{M}), \ldots, (-\varphi_{E_M}^2, \frac{2}{M})\}$. As we can observe, the proposed asymptotic closed-form expression for the ASC is relatively simpler and tractable in relation to the potential solution of Eq. (7), which would fail to provide more insight about the impact of some influential parameters such as the normalized beam width at the receiver-side, the eavesdropper's location and its orientation as well as the number of laser sources at the legitimate transmitter for system design and optimization purposes.

With the goal of exploiting the developed asymptotic closed-form expression to get more insight about the impact of the aforementioned parameters, we can easily compute the extra power required to get a given asymptotic ASC when there is eavesdropper versus no eavesdropper by performing some algebraic manipulations in Eq. (15) as follows

$$L[dB] \triangleq \frac{10 \prod_{k=1}^{M} \varphi_{E_k}^2 \, H_{2+3M,2+M}^{1,2+3M}\left(4\gamma_E \sqrt[M]{F_E} \left(\prod_{k=1}^{M} \frac{A_{E_k}L_{E_k}}{\alpha_{E_k}\beta_{E_k}} \right)^{\frac{2}{M}} \,\middle|\, \begin{matrix} (1,1), (1,1), \xi_1 \\ (1,1), \xi_2, (0,1) \end{matrix} \right)}{\ln(10) \prod_{k=1}^{M} \Gamma(\alpha_{E_k})\Gamma(\beta_{E_k})}. \tag{16}$$

The above expression depends solely on the channel of the eavesdropper and quantifies its contribution to the loss. The mathematical procedure for obtaining the above expression can be seen in greater detail in Appendix A.

4. Numerical Results and Discussion

Now, we provide some numerical results and discussions on how the ASC of terrestrial FSO links is enhanced by deploying multiple lasers at the legitimate transmitter. We evaluate the asymptotic ASC of MISO FSO systems for different turbulent conditions and taking into consideration different severity of pointing errors when the number of lasers sources is equal to $M = \{1, 2, 4, 6\}$. We pay special attention to the location and the orientation of the eavesdropper in order to deeply

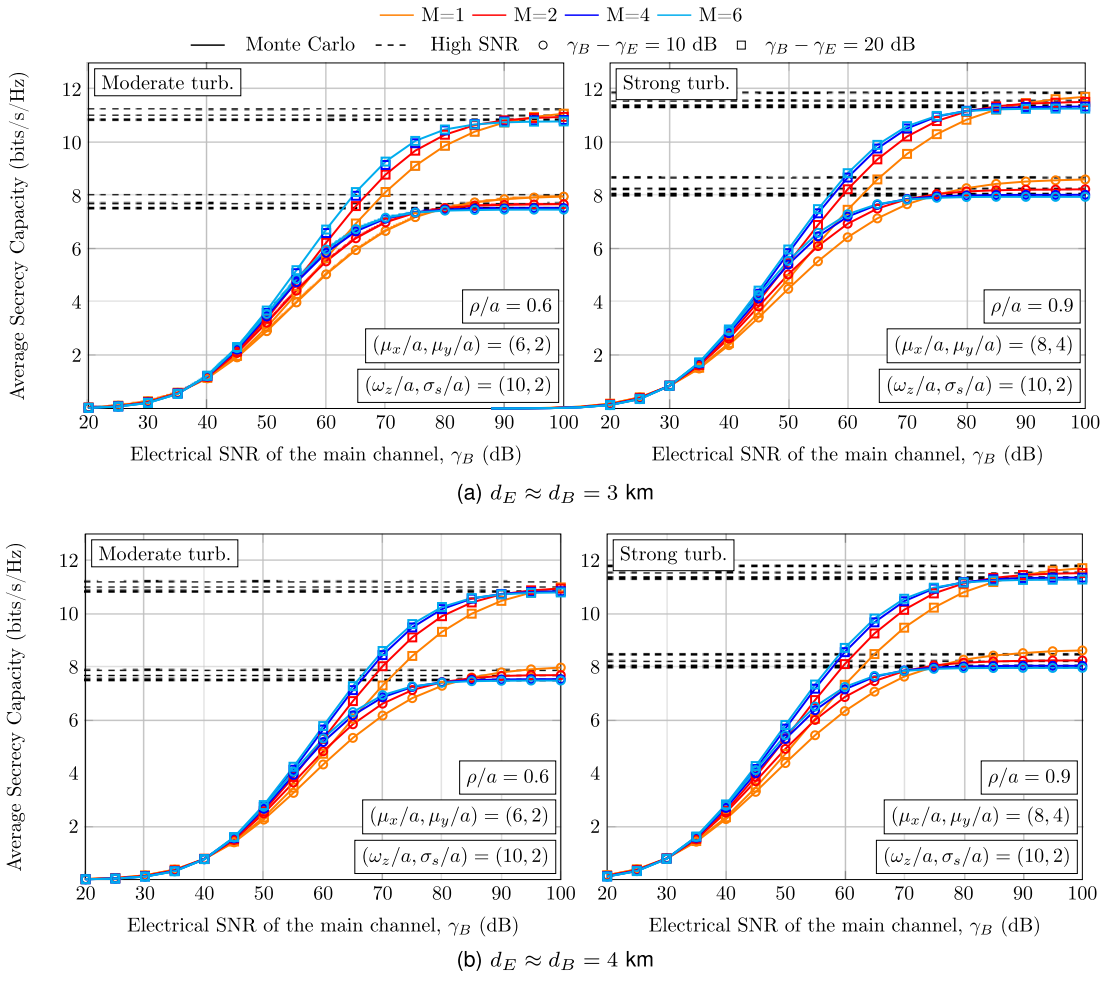

(a) $d_E \approx d_B = 3$ km

(b) $d_E \approx d_B = 4$ km

Fig. 3. ASC of MISO FSO communication systems for an FSO link distance of (a) 3 km, and (b) 4 km as a function of γ_B when $\gamma_E \to \infty$ for different severity of misalignment errors when different weather and turbulent conditions are considered.

analyze the influence of these key parameters on the ASC performance. The FSO system setup under consideration is summarized in Table 1 [21]. In Fig. 2, we depict the ASC for MISO FSO structures as a function of γ_B for different severity of misalignment errors. Besides, the impact of the eavesdropper's location and its orientation is also reflected on this figure by considering the following values: $(\mu_x/a, \mu_y/a, \rho/a) = (6, 2, 0.6)$ and $(\mu_x/a, \mu_y/a, \rho/a) = (8, 4, 0.9)$ for moderate and strong turbulence conditions, respectively. It is evident that the analytical outcomes lead to being in good agreement with the exact Monte Carlo simulations. As a benchmark, we add the ASC performance for a single-transmitter FSO link ($M = 1$), which was derived in [30, Eqs. (9) and (11)]. We observe that the ASC performance is dramatically enhanced because of the employment of multiple lasers at the legitimate transmitter to combat the combined effect of turbulence-induced fading and pointing errors. Interestingly, when pointing errors are not significant, i.e. for small values of σ_s, the capacity of the eavesdropper of capturing radiated power is diminished as a direct consequence of reducing the normalized beam width at the receiver-side. As expected, the ASC for MISO FSO systems increases with the number of laser sources. In Fig. 3, we depict the asymptotic ASC for MISO FSO systems for the same FSO scenario than in the previous figure, but setting $\gamma_B[\text{dB}] - \gamma_E[\text{dB}] = \{10, 20\}$ dB. Surprisingly, we can observe that ASC decreases with increasing the number of laser sources at high SNR, converging to a constant value. The reason

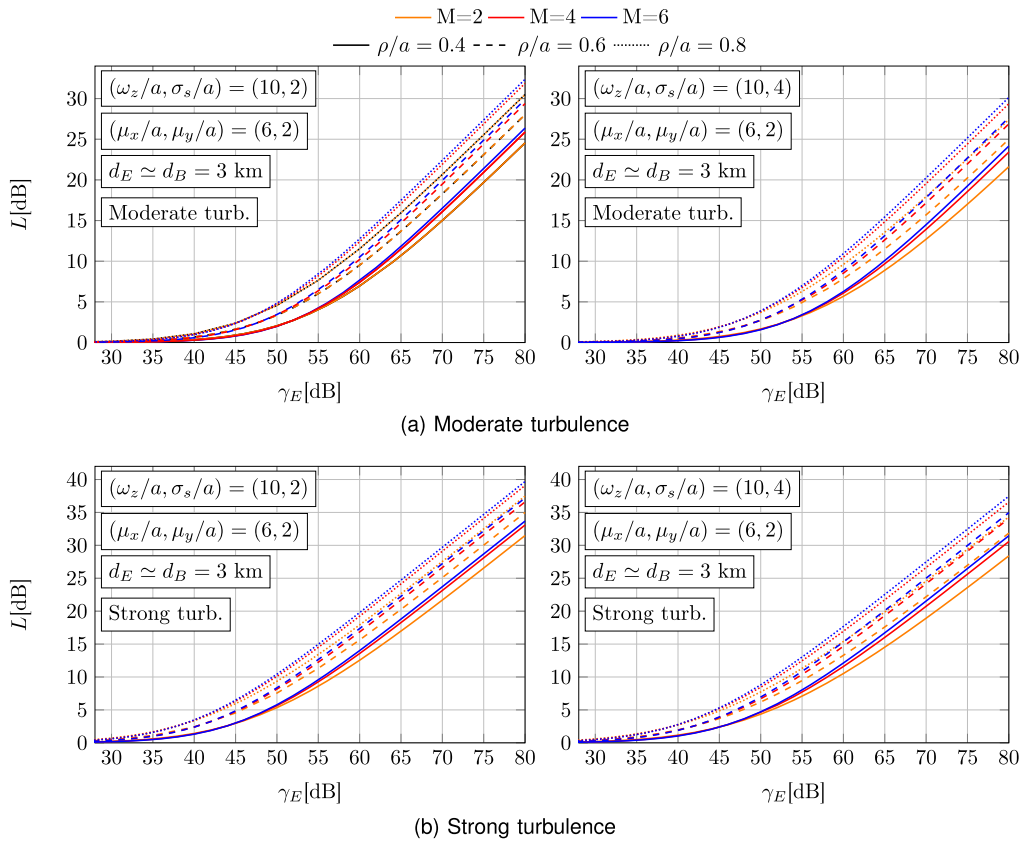

(a) Moderate turbulence

(b) Strong turbulence

Fig. 4. Loss as a function of γ_E for different weather and turbulent conditions when different eavesdropper's locations and different severity of misalignment errors are assumed.

behind this is that both SNR values tend to infinity, and the difference between them is not large enough. Hence, increasing the number of laser sources does not translate into an increase of the achievable secrecy rate when the difference between both SNR values is a constant value. Moreover, it is also observed from Figs. 2 and 3 that the ASC performance slightly decreases as the FSO link distance increases regardless of the number of laser sources under moderate turbulence conditions. However, under strong turbulence conditions, the ASC performance seems to be insensitive when increasing the FSO link distance for the FSO scenario considered under study. Now, the impact of using multiple laser sources at the legitimate transmitter on the secrecy rate is carefully analyzed by exploiting the developed expressions. In Fig. 4, we depict the loss L[dB] as a function of γ_E under different severity of pointing errors of $(\omega_z/a, \sigma_s/a) = \{(10, 2), (10, 4)\}$. We note that this loss increases with γ_E, decreasing the secrecy rate that can be achieved regardless of the number of laser sources and how significant the pointing errors are. The secure transmission is not impaired at all for small values of γ_E since the ASC performance is very close to the performance with no eavesdropper, i.e., $L = 0$ dB. At the same time, we can also observe that the loss increases with increasing the normalized rotation parameter. In other words, the loss is strongly dependent on the eavesdropper's orientation as reflected on the results. In Fig. 5, we depict the loss L[dB] as a function of ω_z/a at the receiver plane for different values of the eavesdropper's orientation of $\rho/a = \{0.4, 0.6, 0.8\}$. Besides, the impact of the eavesdropper's location is also reflected on this figure by considering the following values: $(\mu_x/a, \mu_y/a) = \{(6, 2), (8, 4)\}$. It can be seen that as the normalized rotation parameter increases, i.e. the value of the eavesdropper's orientation, the loss also increases regardless of the number of laser sources. As expected, when

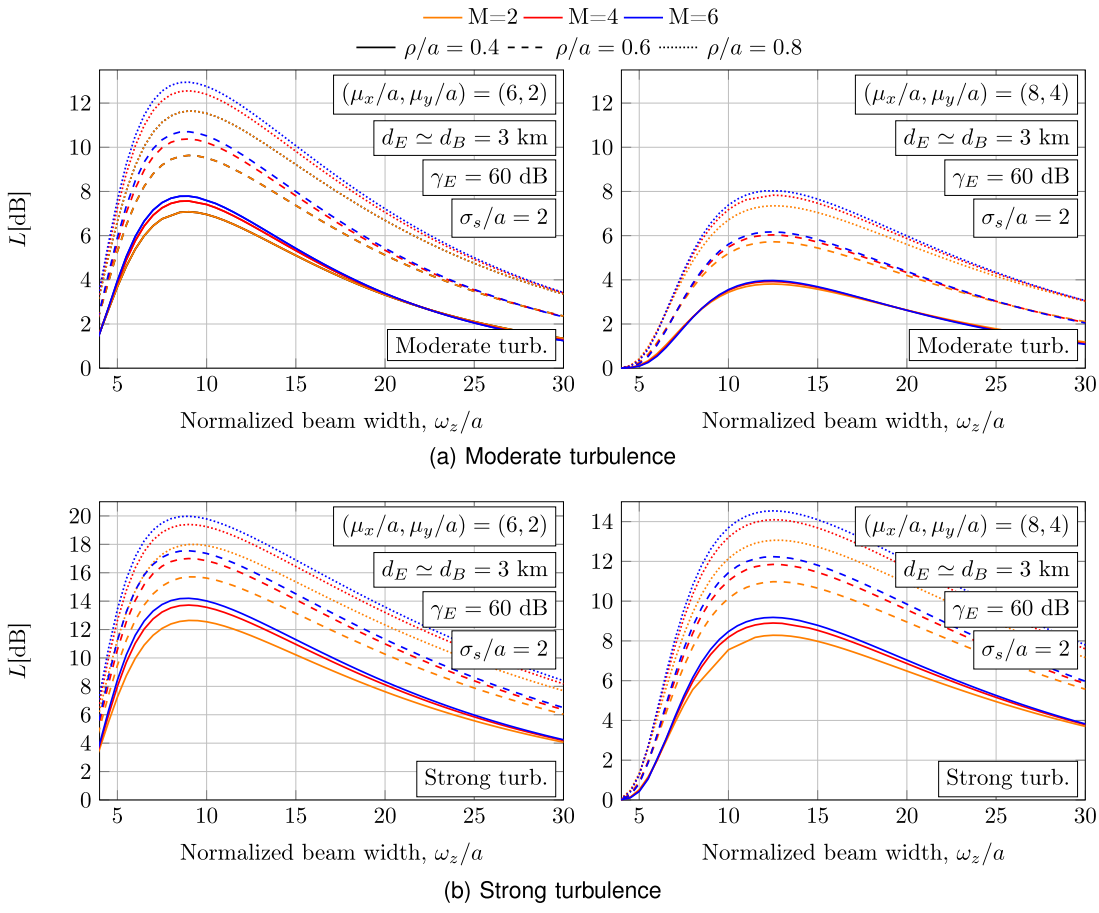

Fig. 5. Loss as a function of ω_z/a for different weather and turbulent conditions when different eavesdropper's locations and different severity of misalignment errors are considered.

the eavesdropper is a little bit further away from the beam center, the required normalized beam width is much less to achieve a given secrecy performance as close as possible to the capacity performance with no eavesdropper. By other hand, as the normalized beam width increases, the influence of the eavesdropper on capturing radiated power is diminished gradually. In other words, the secrecy performance tends to the performance with no eavesdropper as ω_z/a increases. In Fig. 6, we depict the loss L[dB] as a function of μ_x/a when $\mu_y/a = 2$ when different FSO scenarios are studied for moderate and strong turbulence conditions. Note that these results have been obtained for $M = 2$ since this number of laser sources results in being more interesting to analyze in greater detail the impact of some influential parameters on the ASC performance, not obtaining a relevant enhancement for $M > 4$. From Fig. 6, we can conclude that our results provide compelling evidence that the ASC performance of MISO FSO structures depends dramatically on both the location and the orientation of a potential observer. For instance, Figs. 6(a1), 6(a2), 6(b1) and 6(b2) show that the larger normalized rotation parameter and the larger value of γ_E, the closer to the capacity performance with no observer when misalignment errors are not relevant, i.e., for small values of σ_s/a. By other hand, Figs. 6(a3) and 6(b3) show that when misalignment errors become relevant, for $\sigma_s/a = 6$, this can lead to increasing the secrecy rate, allowing the observer to recollect less emitted power. As expected and corroborated from other viewpoints, as the observer gets away from the legitimate receiver, its impact in recollecting radiated power is diminished considerably.

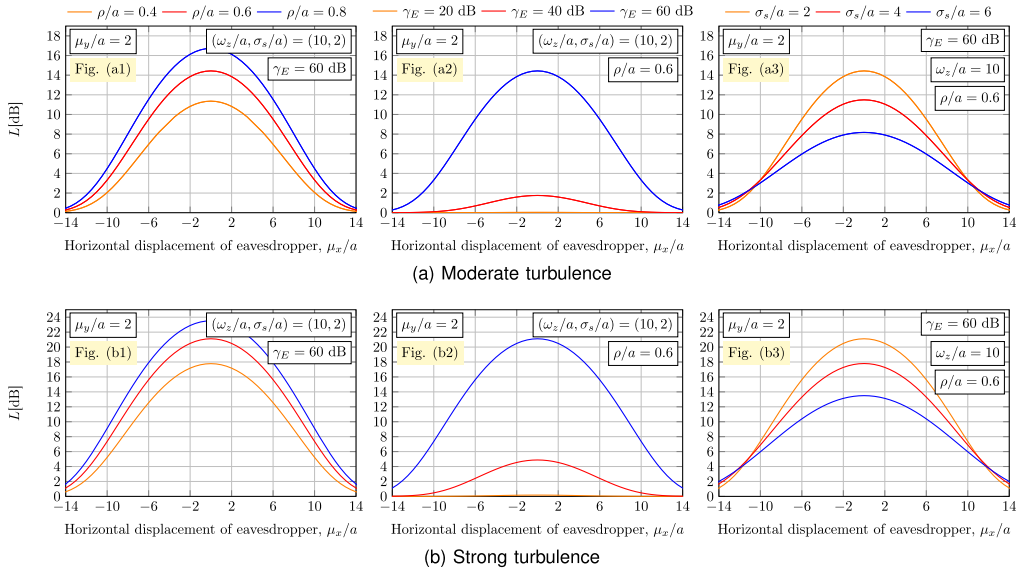

(a) Moderate turbulence

(b) Strong turbulence

Fig. 6. Loss for $M = 2$ as a function of μ_x/a when $\mu_y/a = 2$, and different weather and turbulent conditions as well as different severity of misalignment errors are considered.

5. Conclusion

We have conducted a careful research of the employment of multiple laser sources as a potential measure to remarkably enhance the ASC performance of FSO links. We have analyzed the ASC performance in the presence of turbulence-induced fading channels affected by nonzero boresight pointing errors.

In the light of the results presented here, the use of multiple laser sources results in being an efficient way to guarantee secure transmission in the next generation wireless networks where security issues are becoming more important. Including the impact of the eavesdropper's orientation along with its location in the pointing error model represents an unprecedented milestone in the ASC performance analysis of MISO FSO structures. Both parameters play a crucial role in this kind of performance analysis due to the very highly directive nature of FSO technology. On the other hand, we have also confirmed that a higher secrecy rate can be achieved when deploying structures based on multiple lasers at the transmitter-side, not obtaining a significant performance for $M > 4$ under different turbulence conditions. Indeed, the ASC performance can be improved even in the presence of larger amounts of misalignment. Additionally, the influence of the eavesdropper on capturing radiated power can be diminished notably by increasing not only the normalized beam width at the receiver-side, but also the number of laser sources.

Appendix A

This asymptotic analysis can be extended to get a point where the ASC at high SNR intersects with the γ_B-axis ($\bar{C}_s = 0$ (bits/s/Hz)). This point can be understood as a SNR threshold, i.e. $\gamma^{th}_{B_{eve}}$, in which the ASC starts to significantly increase. From Eq. (15), we can easily express $\gamma^{th}_{B_{eve}}$ in terms of the main and the eavesdropper's channels as follows

$$\gamma^{th}_{B_{eve}}[\text{dB}] = \frac{-20}{\ln(10)}\left(\frac{2\ln(F_B)}{M} + \ln(4) + \frac{2}{M}\sum_{k=1}^{M}\psi(\alpha_{B_k}) + \psi(\beta_{B_k}) - \frac{1}{\varphi^2_{B_k}} - \ln\left(\frac{\alpha_{B_k}\beta_{B_k}}{A_{B_k}L_{B_k}}\right)\right) + \frac{10\prod_{k=1}^{M}\varphi^2_{E_k}\, H^{1,2+3M}_{2+3M,2+M}\left(4\gamma_E\sqrt[M]{F_E}\left(\prod_{k=1}^{M}\frac{A_{E_k}L_{E_k}}{\alpha_{E_k}\beta_{E_k}}\right)^{\frac{2}{M}}\middle|\begin{matrix}(1,1),(1,1),\xi_1\\(1,1),\xi_2,(0,1)\end{matrix}\right)}{\ln(10)\prod_{k=1}^{M}\Gamma(\alpha_{E_k})\Gamma(\beta_{E_k})}. \quad (17)$$

From the above expression, we can easily compute the extra power required to get a given asymptotic ASC when there is eavesdropper versus no eavesdropper as follows

$$L[dB] \triangleq \gamma^{th}_{B_{eve}}[dB] - \gamma^{th}_{B_{no-eve}}[dB]$$
$$= \frac{10\prod_{k=1}^{M}\varphi^2_{E_k} H^{1,2+3M}_{2+3M,2+M}\left(4\gamma_E \sqrt[M]{F_E}\left(\prod_{k=1}^{M}\frac{A_{E_k}L_{E_k}}{\alpha_{E_k}\beta_{E_k}}\right)^{\frac{2}{M}}\middle|\begin{matrix}(1,1),(1,1),\xi_1\\(1,1),\xi_2,(0,1)\end{matrix}\right)}{\ln(10)\prod_{k=1}^{M}\Gamma(\alpha_{E_k})\Gamma(\beta_{E_k})}. \quad (18)$$

Note that $\gamma^{th}_{B_{no-eve}}$ is the SNR threshold with no eavesdropper obtained as

$$\gamma^{th}_{B_{no-eve}}[\text{dB}] = \frac{-20}{\ln(10)} \times \left(\frac{2\ln(F_B)}{M} + \ln(4) + \frac{2}{M}\sum_{k=1}^{M}\psi(\alpha_{B_k}) + \psi(\beta_{B_k}) - \frac{1}{\varphi^2_{B_k}} - \ln\left(\frac{\alpha_{B_k}\beta_{B_k}}{A_{B_k}L_{B_k}}\right)\right). \quad (19)$$

Acknowledgment

The statements made herein are solely the responsibility of the authors.

References

[1] R. Boluda-Ruiz, S. C. Tokgoz, A. García-Zambrana, and K. Qaraqe, "Asymptotic average secrecy rate for MISO free-space optical wiretap channels," in *Proc. IEEE 20th Int. Workshop Signal Process. Advances Wireless Commun.*, 2019, pp. 1–5.
[2] D. Wang, B. Bai, W. Zhao, and Z. Han, "A survey of optimization approaches for wireless physical layer security," *IEEE Commun. Surv. Tut.*, vol. 21, no. 2, pp. 1878–1911, Apr.–Jun. 2018.
[3] M. Bloch, J. Barros, M. R. Rodrigues, and S. W. McLaughlin, "Wireless information-theoretic security," *IEEE Trans. Inf.*, vol. 54, no. 6, pp. 2515–2534, Jun. 2008.
[4] Y. Liang, H. V. Poor, and S. Shamai, "Secure communication over fading channels," *IEEE Trans. Inf. Theory*, vol. 54, no. 6, pp. 2470–2492, Jun. 2008.
[5] L. Wang, M. Elkashlan, J. Huang, R. Schober, and R. K. Mallik, "Secure transmission with antenna selection in MIMO Nakagami-*m* fading channels," *IEEE Trans. Wireless Commun.*, vol. 13, no. 11, pp. 6054–6067, Nov. 2014.
[6] N. Bhargav, S. L. Cotton, and D. E. Simmons, "Secrecy capacity analysis over α-μ fading channels: Theory and applications," *IEEE Trans. Commun.*, vol. 64, no. 7, pp. 3011–3024, Jul. 2016.
[7] H. Lei, I. S. Ansari, G. Pan, B. Alomair, and M.-S. Alouini, "Secrecy capacity analysis over α-μ fading channels," *IEEE Commun. Lett.*, vol. 21, no. 6, pp. 1445–1448, Jun. 2017.
[8] B. Van Nguyen, H. Jung, and K. Kim, "Physical layer security schemes for full-duplex cooperative systems: State of the art and beyond," *IEEE Commun. Mag.*, vol. 56, no. 11, pp. 131–137, Nov. 2018.
[9] M. A. Khalighi and M. Uysal, "Survey on free space optical communication: A communication theory perspective," *IEEE Commun. Surv. Tut.*, vol. 16, no. 4, pp. 2231–2258, Oct.–Dec. 2014.
[10] H. Endo *et al.*, "Free-space optical channel estimation for physical layer security," *Opt. Express*, vol. 24, no. 8, pp. 8940–8955, 2016.
[11] F. J. Lopez-Martinez, G. Gomez, and J. M. Garrido-Balsells, "Physical-layer security in free-space optical communications," *IEEE Photon. J.*, vol. 7, no. 2, Apr. 2015 Art. no. 7901014.
[12] A. H. A. El-Malek, A. M. Salhab, S. A. Zummo, and M.-S. Alouini, "Security-reliability trade-off analysis for multiuser SIMO mixed RF/FSO relay networks with opportunistic user scheduling," *IEEE Trans. Wireless Commun.*, vol. 15, no. 9, pp. 5904–5918, Sep. 2016.
[13] H. Lei, Z. Dai, I. S. Ansari, K.-H. Park, G. Pan, and M.-S. Alouini, "On secrecy performance of mixed RF-FSO systems," *IEEE Photon. J.*, vol. 9, no. 4, Aug. 2017, Art. no. 7904814.
[14] X. Pan, H. Ran, G. Pan, Y. Xie, and J. Zhang, "On secrecy analysis of DF based dual hop mixed RF-FSO systems," *IEEE Access*, vol. 7, pp. 66 725–66 730, 2019.
[15] M. J. Saber and S. M. S. Sadough, "On secure free-space optical communications over Málaga turbulence channels," *IEEE Wireless Commun. Lett.*, vol. 6, no. 2, pp. 274–277, Apr. 2017.
[16] R. Boluda-Ruiz, A. García-Zambrana, B. Castillo-Vázquez, and K. Qaraqe, "Secure communication for FSO links in the presence of eavesdropper with generic location and orientation," *Opt. Express*, vol. 27, no. 23, pp. 34 211–34 229, Nov. 2019.
[17] L. Andrews, R. Phillips, and C. Hopen, *Laser Beam Scintillation With Applications*, vol. 99. Bellingham, WA, USA: SPIE, 2001.
[18] R. Boluda-Ruiz, A. García-Zambrana, C. Castillo-Vázquez, and B. Castillo-Vázquez, "Novel approximation of misalignment fading modeled by Beckmann distribution on free-space optical links," *Opt. Express*, vol. 24, no. 20, pp. 22 635–22 649, Oct. 2016.

[19] R. Boluda-Ruiz, A. García-Zambrana, B. Castillo-Vázquez, and C. Castillo-Vázquez, "On the effect of correlated sways on generalized misalignment fading for terrestrial FSO links," *IEEE Photon. J.*, vol. 9, no. 3, Apr. 2017 Art. no. 7903414.
[20] A. García-Zambrana, R. Boluda-Ruiz, C. Castillo-Vázquez, and B. Castillo-Vázquez, "Novel space-time trellis codes for free-space optical communications using transmit laser selection," *Opt. Express*, vol. 23, no. 19, pp. 24 195–24 211, Sep. 2015.
[21] S. Bloom, E. Korevaar, J. Schuster, and H. Willebrand, "Understanding the performance of free-space optics [invited]," *J. Opt. Netw.*, vol. 2, no. 6, pp. 178–200, 2003.
[22] R. Boluda-Ruiz, A. García-Zambrana, B. Castillo-Vázquez, and C. Castillo-Vázquez, "On the capacity of MISO FSO systems over gamma-gamma and misalignment fading channels," *Opt. Express*, vol. 23, no. 17, pp. 22 371–22 385, Aug. 2015.
[23] I. I. Kim, B. McArthur, and E. J. Korevaar, "Comparison of laser beam propagation at 785 nm and 1550 nm in fog and haze for optical wireless communications," in *Proc. Inf. Technol.*, 2001, pp. 26–37.
[24] A. P. Prudnikov, Y. A. Brychkov, and O. I. Marichev, *Integrals and Series Volume 3: More Special Functions*, vol. 3. Gordon and Breach Science Publishers, 1999.
[25] M. A. Al-Habash, L. C. Andrews, and R. L. Phillips, "Mathematical model for the irradiance probability density function of a laser beam propagating through turbulent media," *Opt. Eng.*, vol. 40, pp. 1554–1562, 2001.
[26] J. Galambos and I. Simonelli, *Products of Random Variables: Applications to Problems of Physics and to Arithmetical Functions*. Boca Raton, FL, USA: CRC Press, 2004.
[27] R. Boluda-Ruiz, A. García-Zambrana, B. Castillo-Vázquez, and C. Castillo-Vázquez, "Impact of nonzero boresight pointing error on ergodic capacity of MIMO FSO communication systems," *Opt. Express*, vol. 24, no. 4, pp. 3513–3534, Feb. 2016.
[28] A. A. Kilbas, *H-Transforms: Theory and Applications*. CRC Press, 2004.
[29] Wolfram Research, Inc. The Wolfram functions site. [Online]. Available: http://functions.wolfram.com
[30] R. Boluda-Ruiz, C. Castillo-Vázquez, B. Castillo-Vázquez, A. García-Zambrana, and K. Qaraqe, "On the average secrecy capacity for FSO wiretap channels with nonzero boresight pointing errors," in *Proc. IEEE 88th Veh. Technol. Conf.*, 2019, pp. 1–5.